applied optics

Crosstalk-free dual-view liquid crystal display using patterned E-type polarizer

Chao Ping Chen,[1,3] Yishi Wu,[1] Lei Zhou,[1] Keyu Wang,[1] Zhonglin Zhang,[1] and Chul Gyu Jhun[2,*]

[1]Smart Display Lab, Department of Electronic Engineering, Shanghai Jiao Tong University, Shanghai, China
[2]School of Green Energy and Semiconductor Engineering, Hoseo University, Asan, Chungnam, South Korea
[3]e-mail: ccp@sjtu.edu.cn
*Corresponding author: cgjhun@hoseo.edu

Received 20 October 2016; revised 13 December 2016; accepted 14 December 2016; posted 14 December 2016 (Doc. ID 279113); published 11 January 2017

We present a dual-view liquid crystal display that allows two faces of the display to be viewed in opposite directions to show different image/video content simultaneously. This device is characterized by a two-domain twisted nematic liquid crystal and a patterned E-type polarizer. Its key optical performance, including the voltage-luminance curve, crosstalk, and viewing angle, has been investigated. When observed at the best viewing angle, the crosstalk between the right and left views is less than 0.07% for all grayscales. In addition, this type of crosstalk can be immune to the misalignment between the polarizers and the liquid crystal layer. For each right/left view, the range of the viewing angle spans roughly 50°.

OCIS codes: (230.3720) Liquid-crystal devices; (120.2040) Displays; (230.0230) Optical devices.

https://doi.org/10.1364/AO.56.000380

1. INTRODUCTION

Dual-view liquid crystal display (LCD) devices are a multipurpose solution that accommodates two distinct viewing cones together in one display. As with multiple viewing angles, different image or video content can be displayed simultaneously on a screen, depending on the viewing direction. As a result of this capability, this technology offers many possibilities that were previously not possible or were at least difficult. Picture two persons sitting in a car. One could see the global positioning system map on the navigator from driver's seat, whereas the other could watch movies from passenger's seat. Likewise, signs in public places become able to showcase more than one advertisement as people go by.

To date, a number of approaches have been proposed for this use. Parallax barriers [1] and lenticular lenses [2] are the most commonly used physical means to route light from different pixels to each independent field of view. However, the noticeably raised cost due to the parallax barrier or lenticular lens would not appeal to many manufacturers. Directional backlight [3,4] directs the light into right and left viewing cones successively. But this necessitates a fast-response liquid crystal (LC), e.g., an optically compensated bend [5] or blue-phase LC [6]. Patterned electrodes [7,8], by inducing inhomogeneous electric fields, tilt LC molecules toward opposite directions, thereby creating right and left viewing cones. The downside is that the aperture ratio is decreased as a result of the dead zones formed nearby the electrodes. Multi-domain alignment [9–11], usually via photo alignment [12] or an ion beam [13], divides a unit pixel into two subpixels, each for a right or left view. Since these two LC subpixels are adjacent to each other, the crosstalk between them is inevitable and more pronounced at higher voltages if designed as a normally black mode.

Motivated by the above issues, we propose a dual-view LCD featuring two-domain twisted nematic (TN) LC cell and patterned E-type polarizer, which is simple in structure and, most importantly, free of crosstalk. In what follows, its operational principle as well as the simulation results are discussed in depth.

2. OPERATIONAL PRINCIPLE

A. Proposed Structure

Figure 1 is a schematic drawing of the proposed structure, where a layer of two-domain TN LC consisting of right-view and left-view subpixels is sandwiched in between a pair of crossed O-type and E-type polarizers [14–16]. The LC molecules of the right-view and left-view subpixels have opposite orientations or rubbing directions, as indicated by the arrows shown in Fig. 1, so they could rotate in opposite fashions upon the application of voltage. Accordingly, the E-type polarizer is patterned with two sets of optical axes (OAs) tilted toward either the right or left viewing cones. Unlike an O-type polarizer, which is more commonly used and whose OA is traverse to its transmission axis (TA), the E-type polarizer has both its OA and TA in the same direction.

1559-128X/17/030380-05 Journal

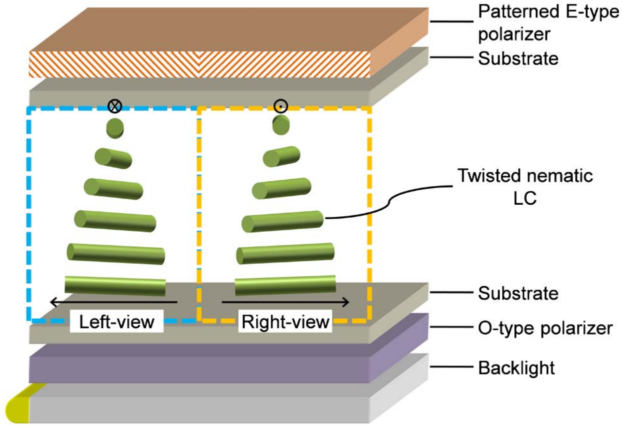

Fig. 1. Proposed structure of dual-view LCD.

B. Normally Black Mode

The proposed dual-view LCD is designed as a normally black mode. To understand its operational principle, we will first, without preference, examine the viewing angle variations of the right-view pixel, as the other half will respond likewise. Referring to Fig. 2(a), a 90° TN LC cell is sandwiched between a pair of O-type and E-type polarizers. The TA of the O-type polarizer is parallel to the LC director at the entrance plane, whereas the TA of the E-type polarizer is perpendicular to the LC director at the exit plane but inclined at a certain angle within the xz plane. In the voltage-off state, the input polarization state will follow the twist of LC directors and be rotated by 90° due to the optical activity [17] caused by the TN LC. As the output polarization state and the TA of the E-type polarizer are mutually orthogonal, the transmission is zero if the Mauguin condition [18] is satisfied. As shown in Fig. 2(b), in the voltage-on state, LC directors—except those near the boundary—are tilted, pointing to a certain angle on the right side at which the transmission reaches its maximum, as the polarization is mostly perpendicular to the LC directors and parallel to the TA of the E-type polarizer at the exit plane. Away from the above angle, the transmittance will gradually decrease.

C. E-Type Polarizer

The E-type polarizer is characterized by its major component, i.e., the negative dichroic dye, which has a larger light absorption coefficient traverse to the OA of the dye than that along the OA of the dye. Let OA be on the x-axis and (θ, ϕ) be the angle of propagation inside the medium of the polarizer, as depicted in Fig. 3. Following Snell's law [17] and the Beer–Lambert law [19], the angular-dependent transmittance of the E-type polarizer can be derived as [20]

$$T_{\parallel} = (1 - R_{\parallel})^2 \cdot \exp\left((\alpha_e \sin^2\theta + \alpha_o \cos^2\theta) \cdot \frac{d}{\cos(\theta)} \right), \quad \textbf{(1)}$$

$$T_{\perp} = (1 - R_{\perp})^2 \cdot \exp\left((\alpha_e \sin^2\theta \sin^2\phi + \alpha_e \cos^2\theta + \alpha_o \sin^2\theta \cos^2\phi) \cdot \frac{d}{\cos(\theta)} \right), \quad \textbf{(2)}$$

$$R_{\parallel} = \left(\frac{-n\cos(\theta_i) + \cos(\theta)}{n\cos(\theta_i) + \cos(\theta)} \right)^2, \quad \textbf{(3)}$$

$$R_{\perp} = \left(\frac{\cos(\theta_i) - n\cos(\theta)}{\cos(\theta_i) + n\cos(\theta)} \right)^2, \quad \textbf{(4)}$$

$$\sin(\theta_i) = n\sin(\theta), \quad \textbf{(5)}$$

where $T_{\parallel,\perp}$ and $R_{\parallel,\perp}$ represent the transmittance and surface reflectance parallel and perpendicular to the incident plane of the light, respectively, θ_i is the incident angle in the air, d is the cell gap, $\alpha_{e,o}$ in turn denotes the extraordinary and ordinary absorption coefficients, and n is the refractive index of the polarizer.

To illustrate the difference between E-type and O-type polarizers, as shown in Fig. 4, the angular dependence of transmittance of a single E-type polarizer and a single O-type polarizer is calculated using the parameters given in Table 1, where E-type and O-type polarizers are idealized as either α_e or α_o and are set as zero. It shall be noted that both E-type and O-type polarizers yield high transmittance for the incidence perpendicular to the OA. For the incidence along the OA, on the other hand, the transmittance of the E-type polarizer drops more dramatically than that of the O-type polarizer, confining the viewing angle to a narrower zone. This disadvantage could be turned into an advantage for multi-view LCDs, where the viewing angle is spatially separated. Consider a case where the viewing angle needs to be limited to the incident angle of 45°. According to Eq. (5), OA has to be inclined by 62° relative to the z-axis.

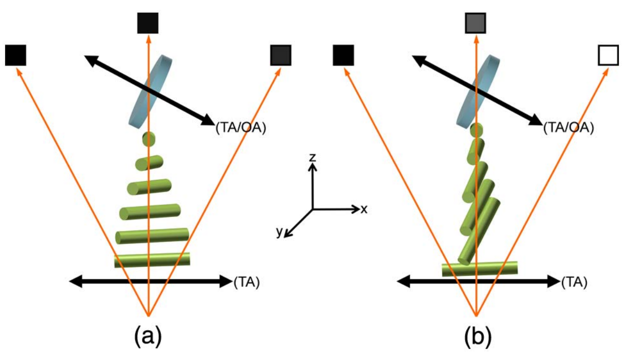

Fig. 2. Illustration of the operational principle: (a) dark state and (b) bright state.

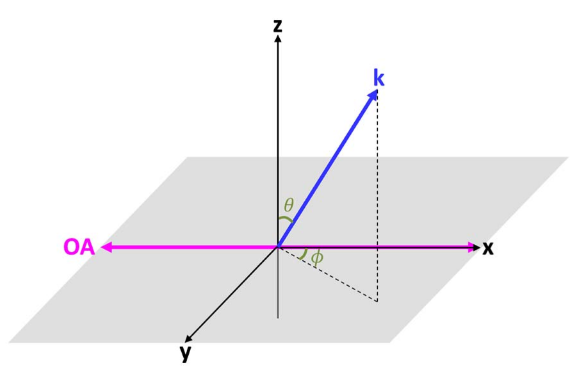

Fig. 3. Orientation of the wave vector and OA of the polarizer.

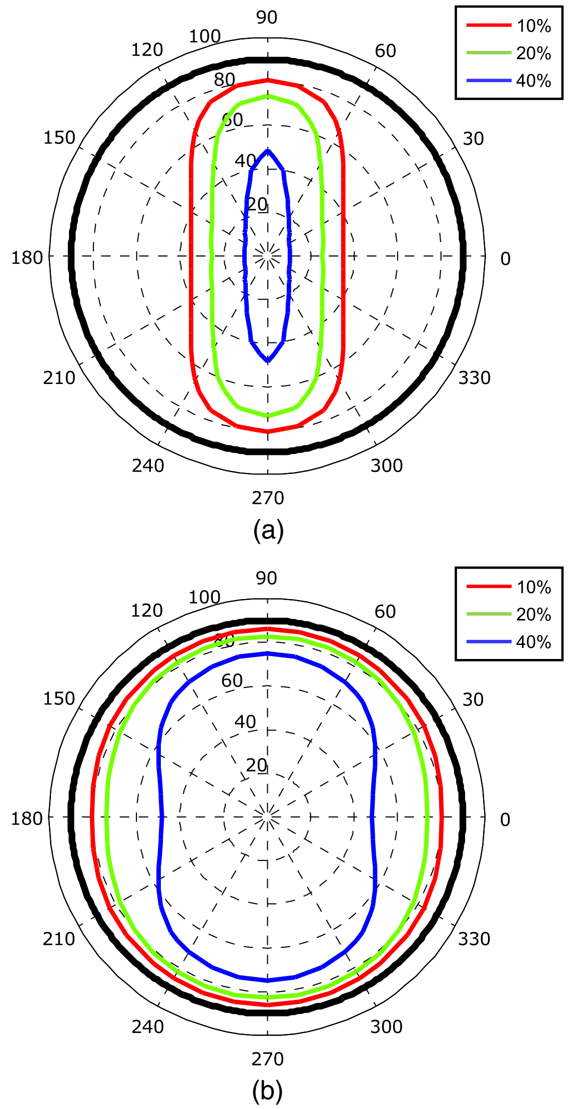

Fig. 4. Calculated angular dependence of transmittance of (a) the single E-type and (b) the single O-type polarizer.

3. RESULTS AND DISCUSSION

A. Simulation Settings

Due to the difficulty of finding negative dyes with a dichroic ratio—the ratio of α_o/α_e—greater than 10:1 [21–23], the device performance is numerically studied with the simulation software DIMOS. Table 2 lists all the parameters used in our simulations. Specifically, the physical properties of the E-type and O-type polarizers are same as those in Table 1, except both OAs are varied in order to achieve the maximum transmittance at the incident angle of 45°. We shall mention that the following results are calculated merely with the right-view pixel, while the left-view pixel is omitted for the sake of clarity. Besides, instead of the transmittance, the luminance—also known as luminous transmittance—that takes into account both the light source spectrum and the International Commission on Illumination color matching functions [24] is calculated over the visible wavelengths ranging from 400 to 700 nm, although the color dispersion [25] is ignored.

Table 1. Parameters Used for the Simulation of E-Type and O-Type Polarizers

Object	Parameter	Value
E-type polarizer	d	100 μm
	n	1.5
	α_e	0 nm^{-1}
	α_o	−0.0001 nm^{-1}
	OA (θ, ϕ)	(90°, 0°)
O-type polarizer	d	100 μm
	n	1.5
	α_e	−0.0001 nm^{-1}
	α_o	0 nm^{-1}
	OA (θ, ϕ)	(90°, 0°)

Table 2. Parameters Used for the Simulation of the Right-View Pixel

Object	Parameter	Value
E-type polarizer	OA (θ, ϕ)	(62°, 0°)
O-type polarizer	OA (θ, ϕ)	(90°, 90°)
LC	d	5 μm
	n_o	1.5
	n_e	1.596
	ϵ_o	4.2
	ϵ_e	8.2
	pretilt	1°
	twist	90°

B. Luminance

Figure 5 plots the voltage-luminance (V-L) curves calculated with respect to incident angles of 0° (front), +45° (45° on the right), and −45° (45° on the left). For +45°, the luminance first monotonically increases to the maximum at 3.1 V—i.e., the bright state—and then starts to decrease, which agrees with the foregoing account of the operational principle. For 0°, the luminance increases at a slower rate and a lower level. For −45°, the luminance stays almost unchanged at a level close to zero regardless of the applied voltage. This can be understood that in either voltage-off or voltage-on state, the polarization of the left-going light is always more or less perpendicular to the OA/TA of the E-type polarizer.

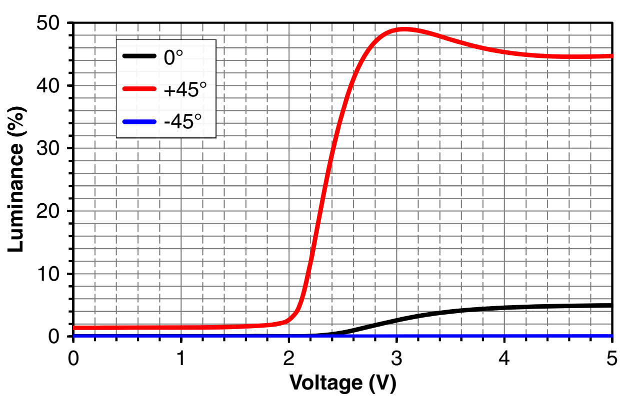

Fig. 5. V-L curves calculated with respect to incident angles of 0° (front), +45° (45° on the right), and −45° (45° on the left).

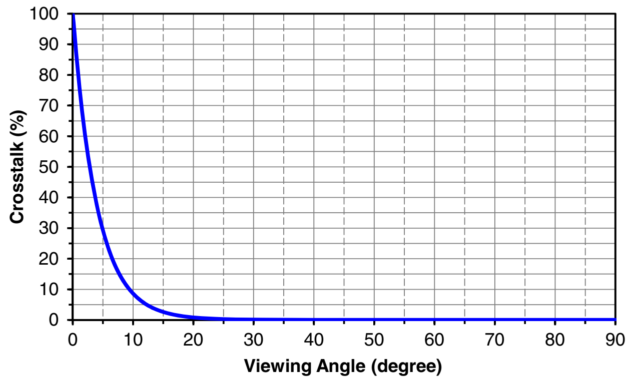

Fig. 6. Crosstalk at the bright state (3.1 V) of the right view against different viewing angles.

C. Crosstalk

Crosstalk [26] is an important indicator for evaluating the performance of dual-view LCDs. It can be defined as [27]

$$\text{Crosstalk} = \frac{\text{Luminance}(L/R)}{\text{Luminance}(R/L)}, \quad (6)$$

where Luminance(L/R) stands for the luminance of the left-view pixel or right-view pixel, or vice versa. Since the left-view and right-view pixels are symmetrical, crosstalk at the bright state (3.1 V) of the right view is calculated against different viewing angles, as shown in Fig. 6. It can be seen that when the viewing angle exceeds 20°, the crosstalk will never go over 1%. In particular, the crosstalk observed at +45° is calculated for voltages varying from 0 to 5 V, as shown in Fig. 7. We find out that, for all voltages or grayscales, the crosstalk stays below 0.07%. With such trivial crosstalk, it can be said that the proposed solution is free from crosstalk for a wide range of both viewing angles and grayscales. Furthermore, even if there is a misalignment between the polarizer and LCD panel, the crosstalk will not be affected. Instead, a loss in the luminance is expected as the aperture ratio becomes smaller.

D. Viewing Angle

The viewing angle characteristics of the dual-view LCD consist of the iso-luminance and iso-contrast ratio (CR) contours. Figure 8 plots the iso-luminance contour of the bright state

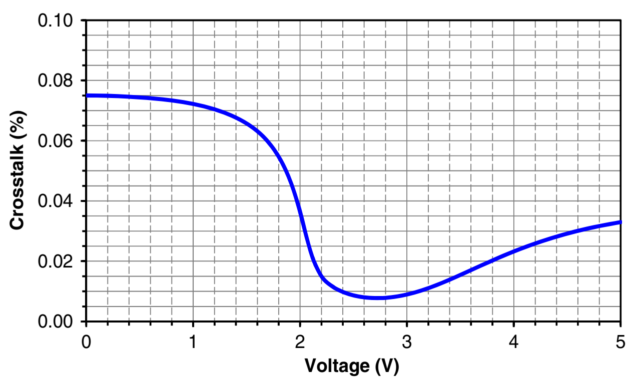

Fig. 7. Crosstalk observed at +45° for voltages varying from 0 to 5 V.

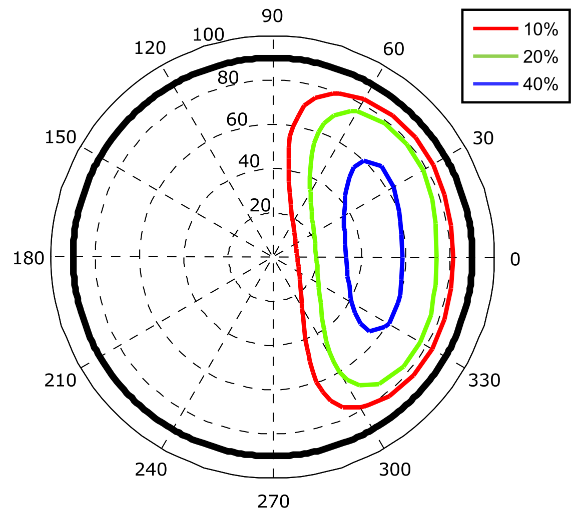

Fig. 8. Iso-luminance contour of the bright state at 3.1 V for levels of 10%, 20%, and 40%.

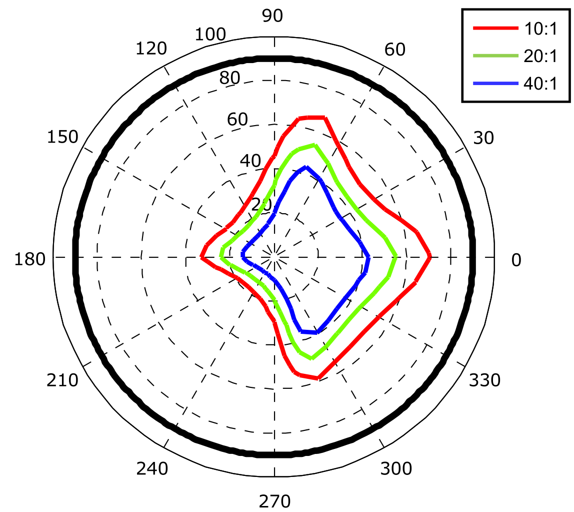

Fig. 9. Iso-CR contour (bright/dark = 3.1 V/0 V) for 10:1, 20:1, and 40:1.

at 3.1 V for levels of 10%, 20%, and 40%. We note that all three levels of luminance are located within the right half of the entire viewing zone. Figure 9 plots the iso-CR contour (bright/dark = 3.1 V/0 V) for 10:1, 20:1, and 40:1. Although part of those CRs intrude on some of the left-half region, the luminance therein is not high enough to display discernible images or even to override the left-view images. Overall, given that crosstalk < 1%, luminance > 10%, and CR > 10, the total viewable window of the right view in the horizontal direction could span roughly 50° (from +20° to +70°).

4. CONCLUSIONS

We have demonstrated a dual-view LCD device that is capable of allowing simultaneous displays via two independent viewing cones on the same screen. The proposed structure features a two-domain TN LC cell and a patterned E-type polarizer, which can eliminate the use of extra viewing angle splitters, e.g., a parallax barrier and lenticular lens. Its key optical performance indicators, including voltage-luminance curve, crosstalk, and viewing angle, have been numerically studied, of which the crosstalk is negligibly small, as compared to its counterparts [7–11]. For practical applications, the proposed dual-view LCD will necessitate the multi-domain alignment and precision panel assembly. The former is technically feasible with photo-alignment technologies [28]. The latter will affect the luminance. But fortunately, the crosstalk can be immune to the misalignment between the polarizers and the LC layer.

Funding. Ministry of Science and Technology of the People's Republic of China (MOST) (2013CB328804, 2015AA017001); National Natural Science Foundation of China (NSFC) (61307028).

REFERENCES

1. J.-Y. Luo, Q.-H. Wang, W.-X. Zhao, and D.-H. Li, "Autostereoscopic three-dimensional display based on two parallax barriers," Appl. Opt. **50**, 2911–2915 (2011).
2. A.-H. Wang, Q.-H. Wang, X.-F. Li, and D.-H. Li, "Combined lenticular lens for autostereoscopic three dimensional display," Optik **123**, 827–830 (2012).
3. J.-P. Cui, Y. Li, J. Yan, H.-C. Cheng, and Q.-H. Wang, "Time-multiplexed dual-view display using a blue phase liquid crystal," J. Disp. Technol. **9**, 87–90 (2013).
4. B.-T. Chen and J.-W. Pan, "Dual-view angle backlight module design," Appl. Opt. **54**, E80–E87 (2015).
5. S. R. Lee, C. G. Jhun, T.-H. Yoon, J. C. Kim, J. D. Noh, D. H. Suh, and J. Y. Lee, "Double-pulse scan of field sequential color driving of optically compensated bend cell," Jpn. J. Appl. Phys. **45**, 2683–2688 (2006).
6. S.-B. Ni, J.-L. Zhu, J. Tan, X.-Y. Sun, E.-W. Zhong, Y.-J. Wang, C. P. Chen, Z.-C. Ye, G.-F. He, J.-G. Lu, and Y. Su, "Critical temperature in phase transition of blue phase liquid crystal," Opt. Mater. Express **3**, 928–934 (2013).
7. C.-T. Hsieh, J.-N. Shu, H.-T. Chen, C.-Y. Huang, C.-J. Tian, and C.-H. Lin, "Dual-view liquid crystal display fabricated by patterned electrodes," Opt. Express **20**, 8641–8648 (2012).
8. C.-T. Hsieh, G.-Y. Li, T.-T. Wu, C.-Y. Huang, C.-J. Tien, K.-Y. Lo, and C.-H. Lin, "Twisted nematic dual-view liquid crystal display based on patterned electrodes," J. Disp. Technol. **10**, 464–469 (2014).
9. C. P. Chen, J. H. Lee, T.-H. Yoon, and J. C. Kim, "Monoview/dual-view switchable liquid crystal display," Opt. Lett. **34**, 2222–2224 (2009).
10. C. P. Chen, T.-C. Chung, X. Guo, and Y. Su, "2-face viewable liquid crystal display by in-plane switching," Mol. Cryst. Liq. Cryst. **544**, 232–236 (2011).
11. C. P. Chen, T.-C. Chung, and T.-S. Jen, "2-face viewable liquid crystal display using 2-domain vertically aligned cell," Photon. Lett. Poland **3**, 23–25 (2011).
12. Q. Guo, A. K. Srivastava, V. G. Chigrinov, and H. S. Kwok, "Polymer and azo-dye composite: a photo-alignment layer for liquid crystals," Liq. Cryst. **41**, 1465–1472 (2014).
13. J. S. Gwag, C. G. Jhun, J. C. Kim, T.-H. Yoon, G.-D. Lee, and S. J. Cho, "Alignment of liquid crystal on a polyimide surface exposed to an Ar ion beam," J. Appl. Phys. **96**, 257–260 (2004).
14. P. I. Lazarev and M. V. Paukshto, "Low-leakage off-angle in E-polarizers," J. Soc. Inf. Display **9**, 101–105 (2001).
15. W. C. Yip, H. S. Kwok, V. M. Kozenkov, and V. G. Chigrinov, "Photo-patterned e-wave polarizer," Displays **22**, 27–32 (2001).
16. P. Lazarev and M. Paukshto, "E-type Polarizers and Retarders," Proc. SPIE **4819**, 46–55 (2002).
17. F. L. Pedrotti, L. M. Pedrotti, and L. S. Pedrotti, *Introduction to Optics* (Addison-Wesley, 2006).
18. P. Yeh and C. Gu, *Optics of Liquid Crystal Displays* (Wiley, 1999), Chap. 5.
19. C. P. Chen, K.-H. Kim, T.-H. Yoon, and J. C. Kim, "A viewing angle switching panel using guest-host liquid crystal," Jpn. J. Appl. Phys. **48**, 062401 (2009).
20. S. E. Han and I. S. Hwang, "Modeling of the optical anisotropy of a dye polarizer," J. Polym. Sci. B Polym. Phys. **40**, 1363–1370 (2002).
21. V. Chigrinov, E. Prudnikova, K. W. Ng, and H. S. Kwok, "Non polarizer guest-host mode based on dyes with negative dichroism," Jpn. J. Appl. Phys. **42**, 1297–1300 (2003).
22. C. P. Chen, H. Li, Z. He, X. Li, Y. Xiong, W. Hu, Y. Su, and C. G. Jhun, "2-face viewable display using dye-doped liquid crystal," SID Symposium **44**, 1380–1383 (2013).
23. V. G. Chigrinov, "Dye, liquid crystals," in *Encyclopedia of Color Science and Technology* (Springer, 2015).
24. A. D. Broadbent, "A critical review of the development of the CIE1931 RGB color-matching functions," Color Res. Appl. **29**, 267–272 (2004).
25. C. P. Chen, C. G. Jhun, S. R. Lee, T.-H. Yoon, J. C. Kim, J. D. Noh, D. H. Suh, and J. Y. Lee, "An alternative OCB mode with reverse-wavelength-dispersion quarter wave plate," in *The 12th International Display Workshops in Conjunction with Asia Display* (ITE/SID, 2005), pp. 133–134.
26. M. Salmimaa and T. Jarvenpaa, "3-D crosstalk and luminance uniformity from angular luminance profiles of multiview autostereoscopic 3-D displays," J. Soc. Inf. Disp. **16**, 1033–1040 (2008).
27. Y.-J. Wu, Y.-S. Jeng, P.-C. Yeh, C.-J. Hu, and W.-M. Huang, "Stereoscopic 3D display using patterned retarder," Soc. Inf. Display Symposium **39**, 260–263 (2008).
28. V. G. Chigrinov, V. M. Kozenkov, and H.-S. Kwok, *Photoalignment of Liquid Crystalline Materials: Physics and Applications* (Wiley, 2008).